

## Article

# Synthesis of Non-Uniform Spiral Antenna with Low Peak Sidelobe Level Using Enhanced Harris Hawks Optimization Algorithm

Tianlong Li <sup>1</sup>, Zhijun Liu <sup>1</sup>, Chen Zhang <sup>2</sup>, Fei Cheng <sup>1</sup>, Yali Yao <sup>3</sup>, Xiumei Li <sup>3</sup>, Haidan He <sup>3</sup> and Yang Yang <sup>1,\*</sup> 

<sup>1</sup> College of Electronics and Information Engineering, Sichuan University, Chengdu 610065, China; tianlongli@stu.scu.edu.cn (T.L.); zjliu@stu.scu.edu.cn (Z.L.)

<sup>2</sup> Anhui Mingbian Electronic Technology Co., No. 66 Yanzihe Road, High-Tech Zone, Hefei 230094, China

<sup>3</sup> The Southwest Institute of Electronic Technology, Chengdu 610065, China

\* Correspondence: yyang@scu.edu.cn

**Abstract:** In this paper, to obtain antenna arrays with grating lobes suppression capability in wide-band and achieve a low peak sidelobe level (PSLL), two non-uniform spiral antenna arrays and an enhanced Harris Hawks optimization (EHHO) algorithm are proposed. By controlling the parameters of the spiral line and sampling equidistant on the spiral line, the sampling points that make up the non-uniform array can be arranged in the plane uniformly and non-uniformly. The simulation results indicate that, because of this special arrangement, the non-uniform arrays obtain the capability of grating lobe suppression in wideband or wide spacing arrangement when compared to the classic uniform array. In addition, to obtain lower PSLL, the Harris Hawks optimization (HHO) algorithm is used for array synthesis because of its diversity of search methods. By employing the step-type taper distribution strategy and the migration strategy, the algorithm's search ability is enhanced, and the simulation results indicate the EHHO algorithm obtains a better solution in terms of the PSLL than other algorithms. A simple patch antenna is designed to build the non-uniform spiral arrays synthesized by the EHHO algorithm. The calculation and simulation results validate the superior performance of the proposed algorithm.

**Keywords:** array synthesis; non-uniform spiral array; Harris Hawks optimization algorithm; grating lobes suppression; peak sidelobe level



**Citation:** Li, T.; Liu, Z.; Zhang, C.; Cheng, F.; Yao, Y.; Li, X.; He, H.; Yang, Y. Synthesis of Non-Uniform Spiral Antenna with Low Peak Sidelobe Level Using Enhanced Harris Hawks Optimization Algorithm. *Electronics* **2024**, *13*, 2959. <https://doi.org/10.3390/electronics13152959>

Academic Editors: Yanki Aslan, Mobayode O. Akinsolu and Maria Kovaleva

Received: 20 June 2024

Revised: 12 July 2024

Accepted: 22 July 2024

Published: 26 July 2024



**Copyright:** © 2024 by the authors. Licensee MDPI, Basel, Switzerland. This article is an open access article distributed under the terms and conditions of the Creative Commons Attribution (CC BY) license (<https://creativecommons.org/licenses/by/4.0/>).

## 1. Introduction

Traditional uniform antenna arrays show good performance in narrowband applications, but in wideband applications, there are issues such as grating lobe, etc., resulting in a decrease in array performance. The non-uniform planar antenna arrays, because of their higher degree of freedom in array arrangement, can suppress grating lobe effectively in the wideband and can obtain larger antenna apertures with smaller elements, which have good prospects in broadband applications. Due to these advantages, methods of designing a non-uniform antenna array with good performance have attracted considerable attention. Traditionally, one approach is to construct thinned arrays [1], which can be designed by removing some elements in a periodic array, and another way is to optimize the positions of elements within a definite aperture size so as to meet the performance requirements [2–6]. In [1], a genetic algorithm (GA) was used to thin the antenna array with the minimization of the side lobe level while maintaining minimal loss of the initial half-power beamwidth. Ref. [7] proposed a method that uses discrete rotated tiles with element positions and optimizes tile orientations to minimize PSLL. In [8], a novel method was proposed whereby social network optimization (SNO) is applied to the optimization of the size of elements to design a reduced-size beam reflectarray. In this paper, based on the Fibonacci spiral and the Archimedes spiral, two non-uniform spiral arrays are presented. The simulation results of

the Fibonacci array (FA) and Archimedes spiral array (ASA) express their excellent effects on grating lobe suppression in broadband and wide spacing arrangements.

The synthesis of an array has the drawbacks of a large calculation range and high time requirements caused by multiple optimization variables. Global optimizations, usually integrated with AI techniques to enhance the computational efficiency, have been developed in the past and have been widely employed in the synthesis of arrays to attack these problems. There are many algorithms, such as the genetic algorithm [9], particle swarm optimization (PSO) algorithm [10,11], simulated annealing (SA) algorithm [12], and mayfly algorithm (MA) [13], etc. [14,15]. MA is a new heuristic algorithm inspired by the flight behavior and the mating process of mayflies, and in [13], it is used to solve the synthesis problem of linear antenna arrays (LAA), obtaining a PSL of  $-35.73$  dB and  $-23.68$  dB for the synthesis of uniform and sparse 32-element LAAs, respectively. In [15], the nonlinear chaotic grey wolf optimization (NCGWO) algorithm was presented to synthesize antenna arrays. The PSL achieved by the NCGWO algorithm was  $-22.4$  dB. Recently, inspired by the unique group predation behavior of Harris Hawks, Heidari proposed a novel heuristic algorithm called the Harris Hawks optimization (HHO) algorithm [16], which has been widely used due to its excellent optimization performance. Therefore, it provides an alternative solution in the synthesis of non-uniform planar arrays. However, for array synthesis, as the number of array elements increases, the solution space, time cost and computational burden increase, leading to a decrease in optimization effect. Moreover, the performance of algorithms greatly depends on the starting point when synthesizing large arrays. Aiming at these problems, in this paper, first, a step-type taper distribution strategy is proposed to provide a good starting point. Then, to improve the capability of global search and prevent early convergence, a global search population (GSP) and migration strategy are proposed, improving the performance of the HHO algorithm. Taking PSL as the optimization objective, the non-uniform antenna arrays were synthesized by several algorithms, and the results show the superiority of the EHHO algorithm.

This paper is organized as follows. In Section 2, the Fibonacci array and Archimedes spiral array are introduced. In Section 3, the HHO algorithm and its improvements are described. In Section 4, the performances of the two non-uniform antenna arrays are tested, followed by the optimization results of different algorithms and the performance comparison, while in Section 5, some conclusions are drawn.

## 2. The Non-Uniform Planar Antenna Arrays

### 2.1. Archimedes Spiral Array

In cases of polar coordinates, the Archimedes spiral can be expressed as follows:

$$\rho = \alpha + \beta * \theta \quad (1)$$

where  $\theta$  is the rotation angle,  $\alpha$  is the distance between the starting point and the origin when  $\theta = 0$ , and  $\beta$  is the spacing control factor, respectively. The distance between two adjacent spirals  $dl$  can be expressed as  $2\pi\beta$ . The ASA comes from the equidistant sampling of an Archimedes spiral. Consider the ASA with  $N$  elements arranged in the  $xy$ -plane, as shown in Figure 1. The coordinates of each element can be expressed as follows:

$$x_i = (\alpha + \beta \times \theta_i) \cos(\theta_i) \quad (2)$$

$$y_i = (\alpha + \beta \times \theta_i) \sin(\theta_i) \quad (3)$$

where  $\theta_i$  can be derived from the following equation:

$$\theta_i = \theta_{i-1} + \arccos\left(\frac{r_i^2 + r_{i-1}^2 - dl^2}{2r_i r_{i-1}}\right), \quad i = 3, 4, 5, \dots, N \quad (4)$$

where  $\theta_i$  is the rotation angle of the  $i$ -th element,  $\theta_1 = 0$ ,  $\theta_2 = 2\pi$ ,  $r_i$  is the distance between the  $i$ -th element and the origin,  $r_1 = 0$ , and  $r_2 = dl$ .

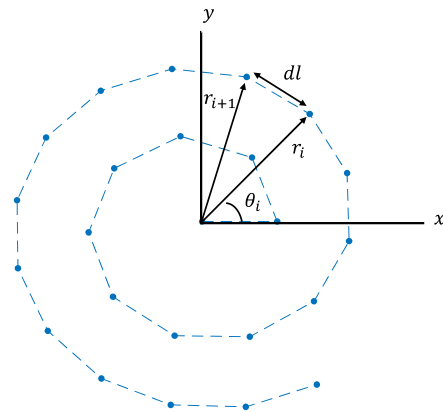


Figure 1. Geometry of the Archimedes spiral array.

### 2.2. Fibonacci Array

Consider the FA with  $N$  elements arranged in the  $xy$ -plane. The elements of the FA generate in turn, and the coordinates of each element can be expressed as follows [17]:

$$x_i = \sqrt{i} \cos(2\pi i \times SF) \tag{5}$$

$$y_i = \sqrt{i} \sin(2\pi i \times SF) \tag{6}$$

where  $i$  is the generation sequence number of the element,  $x_i$  and  $y_i$  are the  $x$ -axis coordinates and  $y$ -axis coordinates of the  $i$ -th element, respectively, and  $SF$  is the structure factor used to control the shape of the FA.

## 3. Enhanced Harris Hawk Optimization Algorithm

In this section, to achieve a lower PSLL for the non-uniform spiral antenna arrays, several improvements are made to the available HHO [16] algorithm. The optimal objective function and the parts of the algorithm improved are formulated, as shown in Equations (6)–(15). Finally, all the processes of the EHHO algorithm are represented.

### 3.1. Fitness Function

Consider the non-uniform array with  $N$  elements arranged in the  $xy$ -plane; the far field pattern  $FP$  can be expressed as the product of the element pattern  $EP$  and the array factor  $AF$  as follows:

$$FP(u, v) = EP(u, v)AF(u, v) \tag{7}$$

$$AF(u, v) = \sum_{i=1}^N A_i e^{jk(d_{ix}u + d_{iy}v)} \tag{8}$$

where  $A_i = a_i e^{j\varphi_i}$  is the excitation of the  $i$ -th element,  $a_i$  is the normalized amplitude,  $\varphi_i$  is the phase;  $k$  is the wave number,  $d_{ix}$  and  $d_{iy}$  are the distances of the elements in the  $x$  and  $y$  direction, respectively,  $u = \sin(\theta)\cos(\varphi)$ ,  $v = \sin(\theta)\sin(\varphi)$ , and  $\theta$  and  $\varphi$  are the elevation and azimuth angles. Thus, taking the PSLL as the optimization objective, the fitness function and the optimization constraint can be expressed as follows:

$$\min Fit = 20 \log_{10} \left( \frac{FP(u(\theta_{psll}, \varphi_{psll}), v(\theta_{psll}, \varphi_{psll}))}{\max(FP(u(\theta, \varphi), v(\theta, \varphi)))} \right) \tag{9}$$

$$s.t. \begin{cases} 0 \leq a_i \leq 1, & i = 1, 2, 3, \dots, N \\ 0 \leq \varphi_i \leq 2\pi, & i = 1, 2, 3, \dots, N \end{cases} \tag{10}$$

where  $\theta_{psll}$  and  $\varphi_{psll}$  correspond to the elevation and azimuth angles of the PSLL. In this paper, all considered arrays have an isotropic element pattern.

### 3.2. Enhanced HHO Algorithm

The HHO algorithm consists of three stages: the global search stage, the transformation stage from global to local, and the local search stage. More details about the HHO algorithm can be found in [16]. In the problem of array synthesis, the solution space expands dramatically as the number of array elements increases, and the global search capability of the algorithm is insufficient to cope with such a large solution space. The optimization effect of the algorithm not only heavily depends on the initial solution, but also easily searches for the local optimal solution instead of the global optimal solution. In this case, on the basis of the original HHO algorithm, two improvements have been made to overcome the shortcomings described above.

Considering that taper distribution can effectively reduce array sidelobe, a step-type taper distribution strategy is proposed, which can be expressed as follows:

$$Y_x = e^{-\alpha x^\beta} \tag{11}$$

$$S_i = [Y_{X_{i-1}} Y_{X_i}] \tag{12}$$

$$a_i \in S_{\text{ceil}(N \cdot r_i / r_{\text{max}})} \tag{13}$$

where  $\beta$  is the taper factor applied to control the degree of variation in taper distribution, and it is a random number in the range  $[0, 4]$ ;  $i$  is the order of step-type and  $N$  is the total order,  $X_i = i/N$ ,  $X_0 = 0$ ,  $S_i$  is the range of the  $i$ -th order's value,  $\text{ceil}$  denotes the upward rounding, and  $r_i$  and  $r_{\text{max}}$  are the distance of the  $i$ -th element from the origin and the furthest distance of the elements from the origin, respectively. The control factor  $\alpha$  is introduced to adjust the range of each order, which varies with the iteration number as follows:

$$\alpha = \alpha_{\text{min}} + \frac{(\alpha_{\text{max}} - \alpha_{\text{min}}) * \text{Gen}}{\text{Gen}_{\text{max}}} \tag{14}$$

where  $\alpha_{\text{min}}$  and  $\alpha_{\text{max}}$  are the minimum and maximum of  $\alpha$ .  $\text{Gen}_{\text{max}}$  and  $\text{Gen}$  are the maximum and current iteration, respectively.

The global search population GSP, which performs a global search based on Equations (11)–(13), and the migration strategy are introduced to enhance the capacity for global search and prevent the algorithm from falling into local optimal solutions. Inspired by the PSO algorithm, the migration strategy consists of two parts. In the first part, after each iteration, the GSP and the SP exchange information with each other, i.e., GSP and SP randomly exchange half of the individual. The second part can be expressed as follows:

Precondition—

$$\text{Fit}_{\text{GSP}_{\text{best}}} < \text{Fit}_{\text{SP}_{\text{best}}}$$

Migration mechanism—

$$X = X + r_1 c_1 (X_{\text{GSP}_{\text{best}}} - X) + r_2 c_2 (X_{\text{SP}_{\text{best}}} - X) \tag{15}$$

where  $\text{GSP}_{\text{best}}$  and  $\text{SP}_{\text{best}}$  are the best individual in GSP and the worst individual in SP, respectively, and  $\text{Fit}_x$  is the fitness of individual  $x$ . Obviously, the smaller the  $\text{Fit}_x$ , the better the PSL.  $X$  is the  $\text{dim}$ -dimensional optimization variable, which is the excitation in array synthesis.  $c_1$  and  $c_2$  are the external factor and internal factor, respectively, and their sum is 1 ( $c_1$  varies according to Equation (14)), representing the impact of GSP and SP on individuals.  $r_1$  and  $r_2$  are  $N$ -dimensional random numbers between 0 and 1. After each iteration, if the fitness of  $\text{GSP}_{\text{best}}$  is better than that of  $\text{SP}_{\text{best}}$ , the individuals of SP perform a migration strategy based on Equation (15).

Based on the above improvements, the EHHO algorithm can be described as follows. Assume that the EHHO algorithm involves a group of  $N_p$  Harris Hawks with a spatial dimension  $\text{dim}$ . In the array, there are NP antenna arrays, each with a number of excitation  $\text{dim}$ . The excitation of the  $i$ th Harris Hawk in the search space is expressed as:

$$IP_i^d = I_i^d + jP_i^d \quad (i = 1, 2, \dots, N_p; d = 1, 2, \dots, \text{dim}) \tag{16}$$

where  $I$  and  $P$  are the amplitude ( $a_i$ ) and phase ( $\varphi_i$ ) of the excitation, respectively. Its excitation distribution can thus be expressed as:

$$IP_i = [I_1, P_1 \ I_2, P_2 \ I_3, P_3 \dots \ I_{dim}, P_{dim}] \tag{17}$$

In the algorithm, some Harris Hawks are selected as a global search population to expand the range of searching and foraging. The remaining individuals serve as the search group. Both groups are initialized according to Equations (11)–(13).

In the global search stage, Harris Hawks randomly inhabit (initialization), and wait to detect prey via on two methods. The opportunity  $q$  for each way is equal, and when  $q < 0.5$ , the positions of Harris Hawks will be changed based on the positions of other members and prey. When  $q > 0.5$ , Harris Hawks will randomly inhabit the trees within the range of activity. The position update equations are

$$IP_{i,d}^t = \begin{cases} IP_{rand,d}^{t-1} - r_1 \left| IP_{rand,d}^{t-1} - 2r_2 IP_{i,d}^{t-1} \right|, q \geq 0.5 \\ \left( IP_{prey,d}^{t-1} - IP_{ave,d}^{t-1} \right) - r_3 (LB + r_4 (UB - LB)), q < 0.5 \end{cases} \tag{18}$$

where  $t$  is the iteration number,  $IP_{i,d}^t$  is the position of the  $i$ th Harris Hawk of the  $t$ th generation in the  $d$ th dimension,  $IP_{prey,d}^{t-1}$  is the position of the prey (i.e., the position of the individual with the best fitness),  $r_1, r_2, r_3, r_4$  and  $q$  are random numbers in the range  $[0, 1]$ ,  $LB$  and  $UB$  are the lower and upper limits of the variables,  $IP_{rand,d}^{t-1}$  is the position of the randomly selected Harris Hawk in the current search population, and  $IP_{ave,d}^{t-1}$  is the average position.

In the transformation stage of global to local, the hunting strategy of the Harris Hawk will be converted based on the escape energy  $E$  of the prey.

$$E = 2E_0 \left( 1 - \frac{t}{T} \right) \tag{19}$$

where  $t$  is the iteration number,  $T$  is the maximum number of iterations, and  $E_0$  is the initial value of escape energy; due to the differences in escape energy between different prey, this last value randomly changes within  $[-1, 1]$  during the iteration process. When  $|E| \geq 1$ , the prey strengthens its activity, so the Harris Hawk searches different areas to further explore the position of the prey, corresponding to the global search stage. When  $|E| < 1$ , The prey weakens its activity, and the Harris Hawk conducts local explorations of adjacent solutions to hunt prey, corresponding to the local search stage.

In the local search stage, it is possible for prey to escape from the Harris Hawks' hunting.  $r$  is the opportunity for the prey to escape before the attack. When  $|E| \geq 0.5$  and  $r \geq 0.5$ , the prey still has enough escape energy, so the Harris Hawks will take measures to further consume the energy of the prey. The position update equations are

$$IP_{i,d}^t = IP_{prey,d}^{t-1} - IP_{i,d}^{t-1} - E \left| J IP_{prey,d}^{t-1} - IP_{i,d}^{t-1} \right| \tag{20}$$

$$J = 2(1 - r_5) \tag{21}$$

where  $J$  is the escape distance of the prey, and  $r_5$  is a random number in the range  $[0, 1]$ . When  $|E| < 0.5$  and  $r \geq 0.5$ , the prey is very tired and has low escape energy. Hard besiege will be used for Harris Hawks to hunt prey. The position update equations are

$$IP_{i,d}^t = IP_{prey,d}^{t-1} - E \left| IP_{prey,d}^{t-1} - IP_{i,d}^{t-1} \right| \tag{22}$$

When  $r < 0.5$  and  $|E| \geq 0.5$ , the prey has a chance to escape from the hunting, and it's escape energy is sufficient. The Harris Hawks hunt through the following two strategies. If the first strategy is ineffective, the second strategy will be executed. The position update equation of the first strategy is

$$Y = IP_{prey,d}^{t-1} - E \left| J IP_{prey,d}^{t-1} - IP_{i,d}^{t-1} \right| \tag{23}$$

The second is

$$Z = Y + S \times LF(dim) \quad (24)$$

where  $S$  is a dim dimensional random vector, and  $LF$  is the Levy flight function [13]. So, the final update strategy for this stage is

$$IP_{i,d}^t = \begin{cases} Y & \text{if } Fit(Y) < Fit(IP_{i,d}^{t-1}) \\ Z & \text{if } Fit(Z) < Fit(IP_{i,d}^{t-1}) \end{cases} \quad (25)$$

When  $r < 0.5$  and  $|E| < 0.5$ , the prey has a chance to escape, but the escape energy is insufficient. To reduce their average distance from the prey, Harris Hawks form a hard enclosure before the raid. The position update equation for this strategy is the same as that in the previous strategy (23)–(25), except for  $Y$ , which can be expressed as follows:

$$Y = IP_{prey,d}^{t-1} - E \left| JIP_{prey,d}^{t-1} - IP_{ave,d}^{t-1} \right| \quad (26)$$

The dimension of the position corresponds to the number of optimization elements in the antenna array. In the process of continuously updating the position, the best optimization scheme for the excitation distribution of the array can be obtained. The steps can be described as Algorithm 1.

---

**Algorithm 1.** EHHOA Synthesis Procedure

---

- 1: Set the population size  $N_p$ , the global search population factor  $P_N = 0.5$ , the number of global search population  $N_{GSP} = N_p \cdot P_N$ , the number of search population  $N_{SP} = N_p \cdot (1 - P_N)$ , the order of the step-type taper distribution strategy  $N = 16$ , the range of the control factor  $\alpha$  ( $\alpha_{min} = 0$ ,  $\alpha_{max} = 4$ ), the lower and upper bounds  $LB$  and  $UB$  of variables, dimension  $dim$  (the element number of antenna array) of the objective function, and the maximum number of iterations  $T$ ;
  - 2: Use the step-type taper distribution strategy to initialize the  $I$  of the global search population and search population, and initialize the  $P$  to 0;
  - 3: Calculate the fitness value of the current Harris Hawk individual, i.e., the PSL of the current array antenna; record the current optimal fitness of two populations  $Fit_{GSP\_best}$  and  $Fit_{SP\_best}$  (the best one will be considered the prey) and the best position  $IP_{best}$ ;
  - 4: **while**  $t \leq T$  **do**
  - 5: Exchange of individuals in GSP and SP according to the migration strategy;
  - 6: **if**  $Fit_{GSP\_best} < Fit_{SP\_best}$  **do**
  - 7: Update the positions of the search population by (15);
  - 8: **else do**
  - 9: Update  $E$ ,  $r = rand(1)$ ;
  - 10: **if**  $|E| \geq 1$  **do**
  - 11: Update the positions of the search population by (18);
  - 12: **else if**  $|E| \geq 0.5$  and  $r \geq 0.5$  **do**
  - 13: Update the positions of the search population by (20);
  - 14: **else if**  $|E| < 0.5$  and  $r \geq 0.5$  **do**
  - 15: Update the positions of the search population by (22);
  - 16: **else if**  $|E| \geq 0.5$  and  $r < 0.5$  **do**
  - 17: Update the positions of the search population by (23)–(25);
  - 18: **else if**  $|E| < 0.5$  and  $r < 0.5$  **do**
  - 19: Update the positions of the search population by (24)–(26);
  - 20: **end if**
  - 21: Update the positions of the global search population by (11)–(13);
  - 22: If the new individual's fitness is better than the previous generation's, update fitness and position;
  - 23:  $t = t + 1$ ;
  - 24: **end while**
  - 25: **return**  $IP_{best}$
-

### 3.3. Performance

Computational efficiency is a critical aspect of the optimization algorithm. The time complexity of the EHHO algorithm is analyzed as follows. In the EHHO algorithm, the most time-consuming operation is the iterative update, because the fitness value of each individual will be calculated at each iteration, and according to Equations (7) and (8), the calculation of the fitness value is accomplished through the cyclic superposition of elements' patterns. We assume that the algorithm undergoes  $N$  iterations, and the optimized array has  $N_a$  elements. If the calculation time of the superposition of each element's pattern is  $T$ , the time required for the algorithm to run once can be expressed as:

$$T_{sum} = N_p \times N \times N_a \times T + T_1 \quad (27)$$

where  $T_1$  represents the low order (about  $N$ ) and constant, and  $N_p$  represents the number of individuals in the population. The low order, constant, and coefficient in the formula do not change the trend of growth; therefore, the time complexity of the EHHO algorithm is proportional to the product of the iterations  $N$  and the antenna elements  $N_a$ , and can be expressed as:

$$O(N \times N_a) \quad (28)$$

It is necessary to manage the computational overhead of the algorithm, which helps to improve the efficiency of the algorithm. Optimization will gradually converge with iterations, so setting appropriate iterations  $N$  can effectively reduce overhead. In addition, parallel processing techniques can be utilized to decompose tasks into multiple subtasks for parallel execution, in order to improve efficiency.

The EHHO algorithm is designed for the synthesis of non-uniform spiral antenna to achieve low PSL. The core of the fitness function of the EHHO algorithm is the superposition principle of the electrostatic field, so the algorithm is suitable for various antennas that can use the principle. Moreover, by changing the optimization objective, the algorithm can be used for other optimization problems, such as special radiation shapes, etc.

## 4. Numerical Results

In this section, firstly, to verify the performance of grating lobes suppression in the wideband of the two non-uniform spiral antenna arrays, the two arrays and the traditional uniform array are arranged in the same size plane with the same amounts of elements, and the PSLs of the three arrays at various frequencies are calculated. Moreover, the PSLs of the two arrays are calculated when the element spacing increases (the number of elements remains unchanged and the size of the arranged plane increases). Next, the EHHO algorithm and other algorithms are used to synthesize the two arrays to reduce PSL, and the optimization results are compared to verify the high performance of the EHHO algorithm. A simple patch antenna is designed to construct the array, and full-wave simulation is conducted to verify the effectiveness of the algorithm.

### 4.1. Arrays Simulations

In this section, we consider an ASA and an FA with 324 elements distributed on the  $10\lambda_0 \times 10\lambda_0$  ( $f_0 = 1$  GHz) plane, as shown in Figure 2. The  $SF$  of the FA is set as the golden ratio  $(\sqrt{5} - 1)/2$ . Figure 3a presents the results of the PSLs from  $f_0$  to  $100f_0$ , obtained from the simulation of the ASA and FA. Note that the amplitude and phase of every element are set as 1 and 0 in the simulation. From Figure 3a, it can be derived, for the classic uniform array arranged periodically, that the grating lobe emerges, because the distance between elements gradually exceeds  $0.5\lambda_0$  as the frequency increases. However, for the ASA and the FA, no grating lobe appears, even though the frequency has increased to  $100f_0$ . As shown in Figure 3a, the PSLs of the FA remain stable at about  $-15$  dB, while for the ASA, the PSLs remain in the range of  $-12$  dB to  $-15$  dB, which values are lower than  $-10$  dB in [18] and  $-12$  dB in [7]. Figure 3b shows the PSLs of the ASA and the FA with different array lengths and the same number of elements (324). It can be seen that the two non-uniform

planar arrays achieve low PSLL (about  $-12$  dB and  $-15$  dB, respectively), despite the array length  $L$  expanding to  $200\lambda_0$  (the minimum distances between the elements of ASA and FA are  $10.21\lambda_0$  and  $8.96\lambda_0$ , respectively), while in [7], the PSLL (higher than  $-10$  dB when  $L = 18\lambda_0$ ) increases as the array length expands. All of these above-mentioned results indicate that the two non-uniform planar arrays have a good capacity for grating lobe suppression in the wideband or wide spacing.

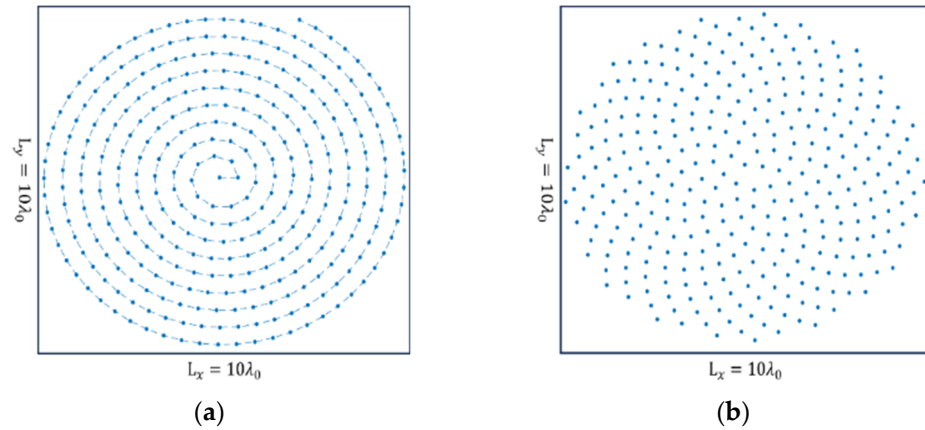


Figure 2. (a) Archimedes spiral array and (b) Fibonacci array.

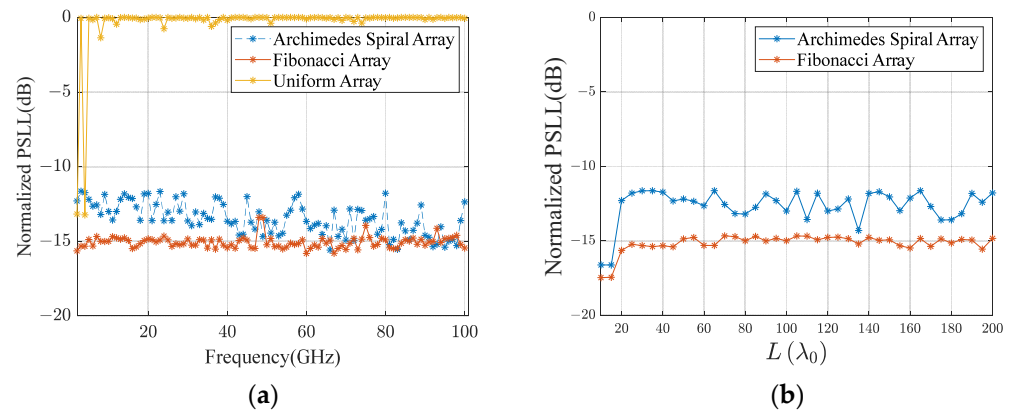


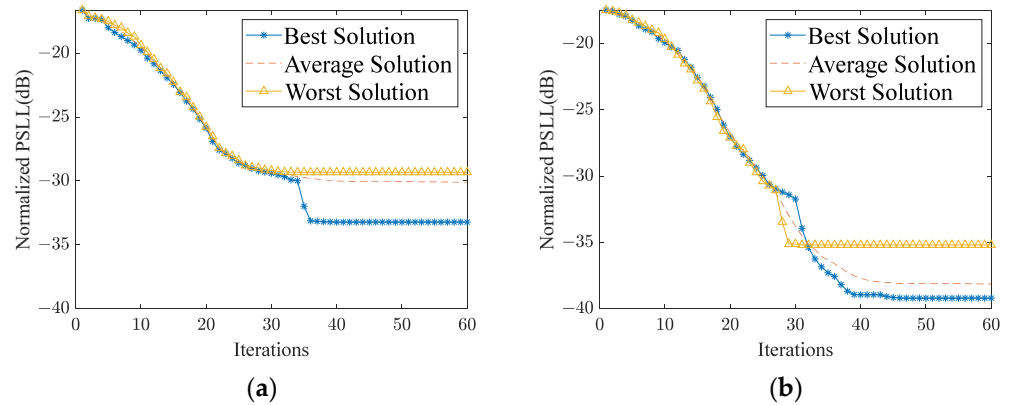
Figure 3. The PSLs of (a) arrays from  $f_0$  to  $100 f_0$  with the direction of  $\theta_0 = 0$  and (b) arrays arranged on planes of different lengths.

#### 4.2. Synthesis of Arrays

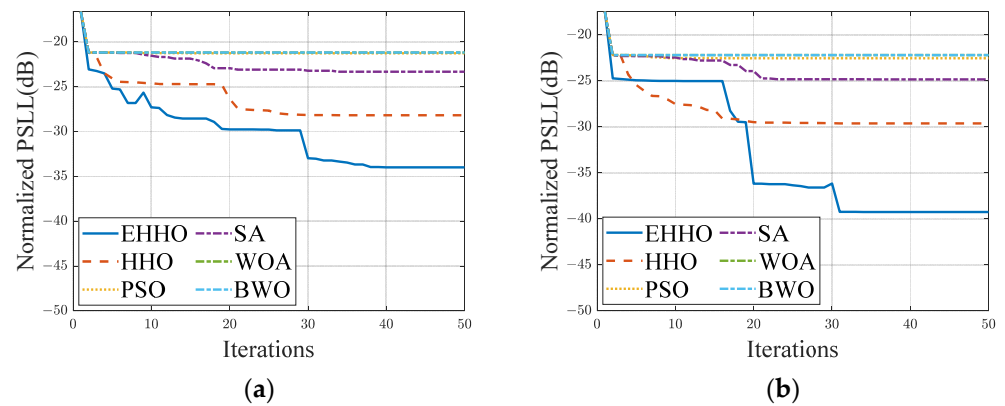
In this section, to demonstrate the superiority of the proposed EHHO algorithm, the SAS and FA are synthesized using the classical PSO, SA, BWO [19], WOA [20], HHO and EHHO. The population size is chosen as 20, and the iteration step is 60. For fairness, the population sizes of GSP and SP in the EHHO algorithm are set as 10, respectively. For the EHHO algorithm, the control parameter  $\beta$  is set through a series of experiments, which randomly change between 0 and 5 in each iteration, and  $\alpha_{min}$  and  $\alpha_{max}$  are set as 0 and 5, respectively. The initial values of the parameters  $\alpha$ ,  $\beta$ ,  $c_1$ , and  $c_2$  are set as 5, 5, 0.5, and 0.5, respectively.

Figure 4 provides the convergence characteristics after 50 independent runs of the EHHO algorithms. The averaged optimal PSLs of ASA and FA are  $-30.1$  dB (0.8 dB lower than the worst  $-29.3$  dB and 3.1 dB higher than the best  $-33.2$  dB) and  $-38.1$  dB (2.9 dB lower than the worst  $-35.2$  dB and 1.1 dB higher than the best  $-39.2$  dB), respectively. Then, the ASA and FA are synthesized by PSO, SA, WOA, BWO, HHO and EHHO, and the convergence characteristics are shown in Figure 5. Table 1 presents a comparison of the results of PSLs obtained by those algorithms. From Figure 5, it can be seen that the optimization effect of these algorithms is limited because of the large solution space. The

algorithm that obtained the optimum PSL is EHHO. From the convergence characteristics and optimal result of the EHHO algorithm, it can be seen that the optimization effect of the HHO algorithm is improved. Specifically, for the synthesis of ASA and FA, the EHHO realizes the optimum PSL, which is 6 dB and 8.5 dB lower than that of HHO (lower than other algorithms), respectively, and lower than the  $-17.78$  dB in [11] and  $-30.38$  dB in [13]. Figure 6 depicts the normalized radiation patterns of ASA and FA obtained by using different algorithms.



**Figure 4.** Convergence characteristics of the EHHO algorithms in the synthesis of (a) Archimedes spiral array and (b) Fibonacci array.



**Figure 5.** Convergence characteristics of the algorithms in the synthesis of (a) Archimedes spiral array and (b) Fibonacci array.

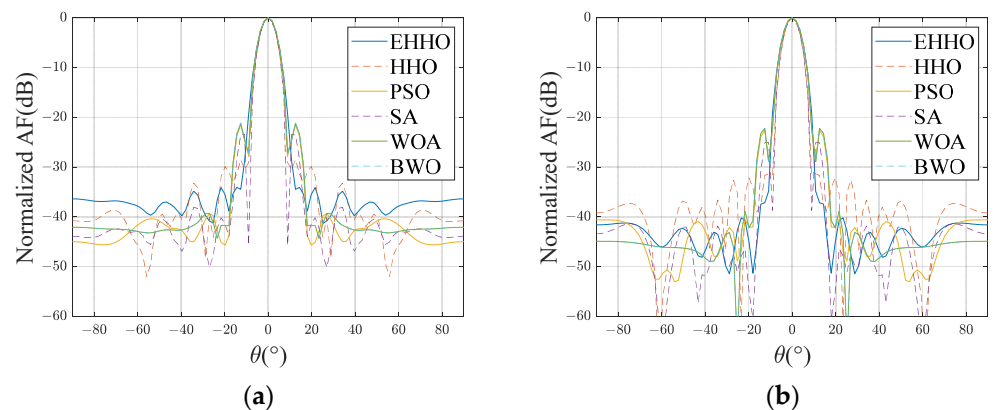


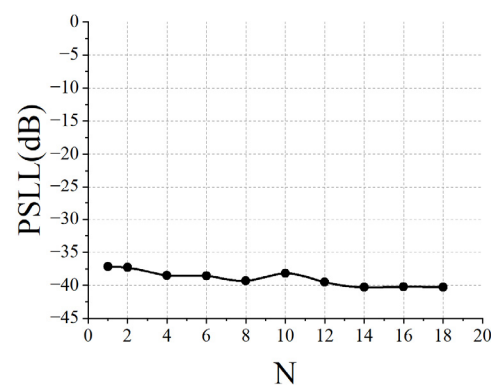
**Figure 6.** Normalized radiation patterns ( $\varphi = 0^\circ$ ) of (a) Archimedes spiral array and (b) Fibonacci array.

**Table 1.** Synthesis results of non-uniform arrays with different algorithms.

Arrays	PSLL (dB)					
	PSO	SA	WOA	BWO	HHO	EHHO
ASA	−21.1	−23.3	−21.1	−21.1	−28.1	−34.1
FA	−22.5	−24.8	−22.2	−22.2	−29.6	−38.1

With the addition of two improvement strategies, the search method of the algorithm increases, the ability to jump out of local optimal solutions and the search ability in the large solution space are enhanced, and the problem of initial value dependence is solved to some extent. These above-mentioned results effectively demonstrate the superior performance of the EHHO algorithm when used in large non-uniform planar array synthesis.

The original HHO algorithm's optimization results are sensitive to initial values. To overcome this drawback, the step-type taper distribution strategy is introduced, as shown in Equations (11)–(14). The EHHO algorithm no longer relies on initial values, but it is necessary to study the impacts of parameter settings in the strategy on optimization. The key parameter in the taper strategy is the total order  $N$  (as shown in Equation (13)). Figure 7 shows the optimization results of the EHHO algorithm with different  $N$  (optimizing the array shown in Figure 2b, all other parameters remain consistent except  $N$ ). From Figure 7, it can be seen that a decrease in  $N$  makes the PSLL increase; when  $N$  is 1, the PSLL is  $-37.2$  dB, while when  $N$  is 14, the PSLL is  $-40.1$  dB. In addition, when  $N$  is greater than 14, the PSLL tends to stabilize. Although the variation in  $N$  affects the optimization results, the impact is within acceptable limits. A conclusion that the EHHO algorithm has good stability and reliability can be drawn.

**Figure 7.** The optimization results of the EHHO algorithm with different  $N$ .

#### 4.3. Simulation Results

To assess the reliability of the proposed algorithm, an experiment on a full-wave simulation model is carried out using the full-wave electromagnetic field solver HFSS as the simulation tool. A simple rectangular microstrip patch is designed as the element structure, as shown in Figure 8a. The width of the patch  $W_p$  is 15.7 mm and the length of the patch  $L_p$  is 11.59 mm. To achieve good impedance matching, the inner core radius of 0.635 mm ( $R_{in}$ ) and a dielectric layer radius of 2.05 mm ( $R_{out}$ ) are designed for the coaxial feed. The distance between the feeding and the edge of the patch is 2.295 mm ( $L_d$ ). The antenna element is printed on an FR4 sheet with a thickness of 1 mm (the relative dielectric constant is 4.4, the loss tangent is 0.02). The performance of the element is shown in Figure 8d, and it operates at 5.8 GHz with a peak gain of 5.4 dBi.

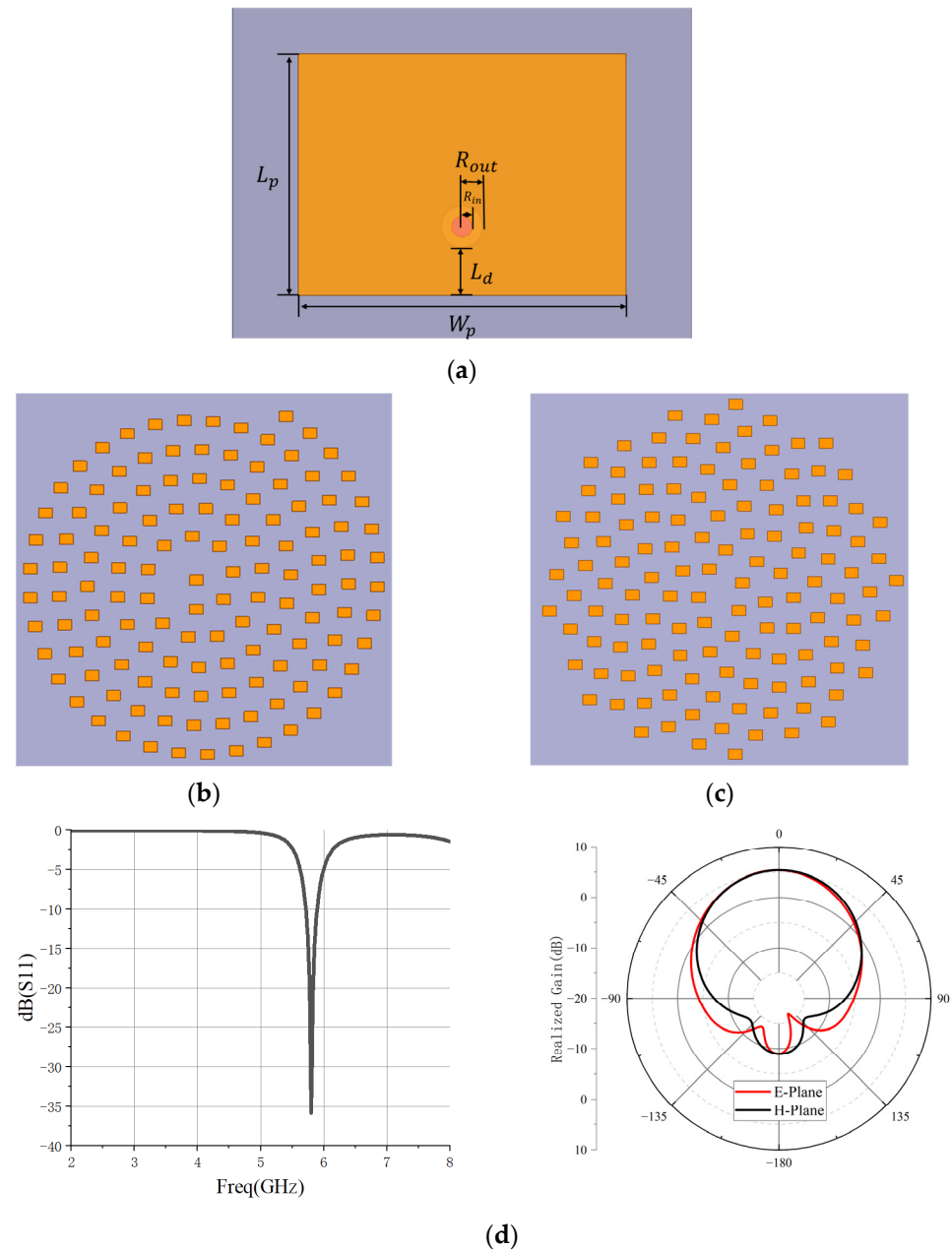


**Figure 8.** Array element used in simulation: (a) patch model; (b) 128-element Archimedes spiral array; (c) 128-element Fibonacci array; (d) S11 and Radiation patterns in the E-plane and H-plane.

In this experiment, a 128-element FA and a 128-element ASA are chosen as the reference, and the simulation model is established in Figure 8b,c with an array size of  $400 \times 400 \text{ mm}^2$ . Due to the influence of edge effects and electromagnetic coupling among elements, there are certain differences in the patterns of each element in the actual finite arrays. Therefore, the AEP (active element pattern) method is used in the actual array pattern synthesis. Firstly, this method simulates and calculates the pattern of each element separately excited (i.e., other elements connected to matching loads without excitation). Then, using the superposition principle of the electrostatic field and the EHHO algorithm, the patterns of all elements are superimposed to obtain the total radiation pattern of the array. The radiation patterns of the FA and ASA synthesized by the EHHO algorithm and simulated by HFSS are shown in Figures 9 and 10, respectively. Comparisons of the performance between calculation and simulation are presented in Table 2. Two cuts of radiation patterns of Fibonacci array and Archimedes spiral array are shown in Figures 11 and 12.

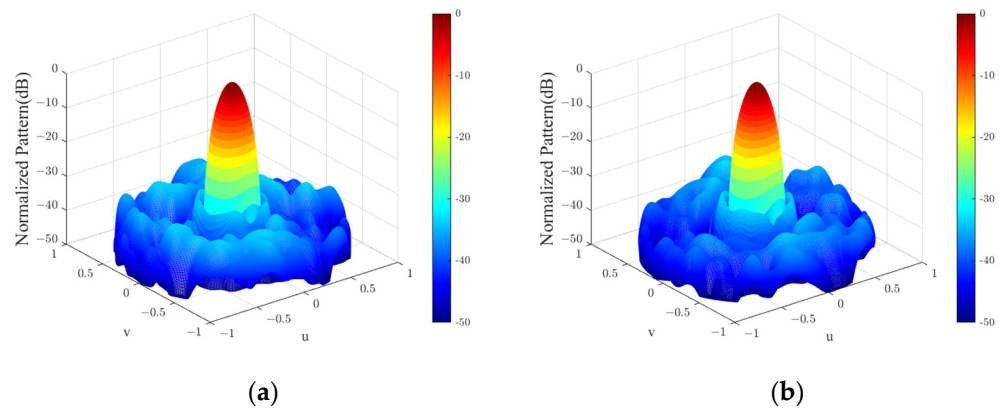


Figure 9. The 3D pattern of the Fibonacci array given by (a) calculation and (b) simulation.

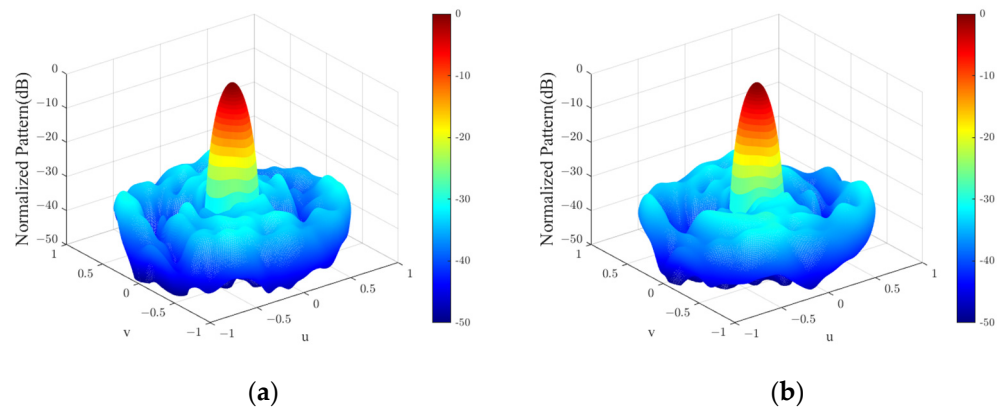


Figure 10. The 3D pattern of the Archimedes spiral array given by (a) calculation and (b) simulation.

Table 2. Calculation and simulation performance comparison.

Array	Result	Calculation	Simulation	Error
Fibonacci array	PSLL (dB)	-33.19	-32.83	0.36
	Gain (dBi)	23.32	23.31	-0.01
Archimedes spiral array	PSLL (dB)	-30.7	-30.3	0.4
	Gain (dBi)	23.44	23.43	-0.01

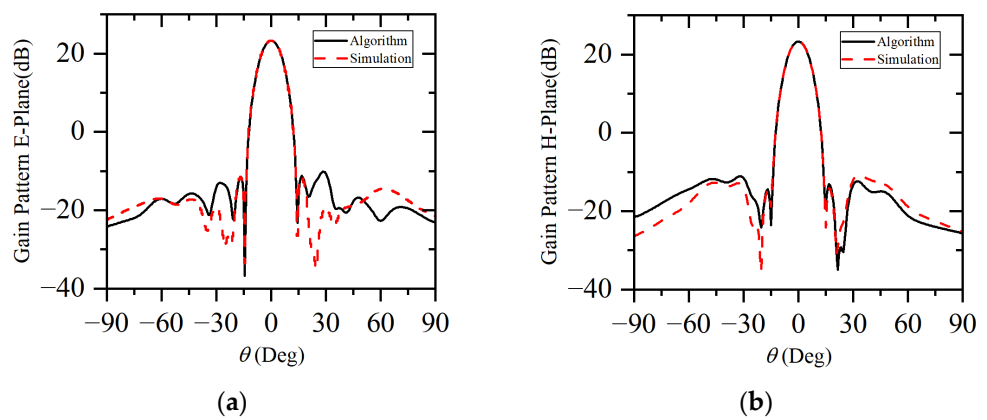
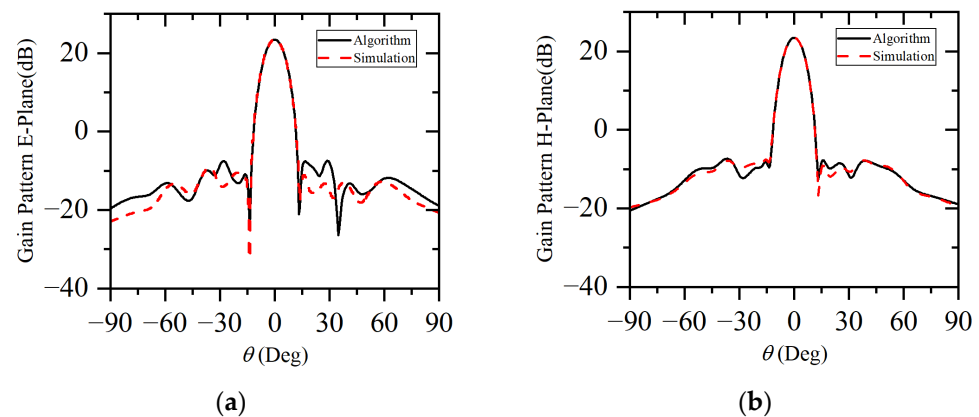


Figure 11. Two cuts of radiation patterns of Fibonacci array: (a)  $\varphi = 0^\circ$  and (b)  $\varphi = 90^\circ$ .



**Figure 12.** Two cuts of radiation patterns of Archimedes spiral array: (a)  $\varphi = 0^\circ$  and (b)  $\varphi = 90^\circ$ .

The simulation results show that the PSLL of the FA and ASA in the upper half of the space are  $-32.83$  dB and  $-30.3$  dB. It increased by  $0.36$  dB and  $0.4$  dB compared to the PSLL values of  $-33.19$  dB and  $-30.7$  dB, respectively, theoretically calculated as the limits of what the arrays can achieve, caused by the mutual influence between elements. The peak gain of the simulation drops to  $23.31$  dBi and  $23.43$  dBi, respectively, corresponding to the same difference of  $0.01$  dBi compared with the calculation. The low difference of the peak gains and PSLLs obtained from the calculation and simulation indicates the effectiveness and reliability of the algorithm.

## 5. Conclusions

Designing non-uniform planar antenna arrays with grating lobe suppression in the wideband and achieving lower peak sidelobe levels are challenging problems. In this paper, we proposed two non-uniform spiral antenna arrays with grating lobe suppression capabilities in the wideband and proposed an enhanced Harris Hawks optimization algorithm for the synthesis of spiral antenna arrays to achieve low PSLL. The experiments have validated that the proposed arrays have the capacity for grating lobe suppression in broadband or wide spacing. To solve the problems of algorithm optimization, such as relying on initial values and easily getting stuck in local optima, we proposed two improvement strategies: the step-type taper distribution strategy and the migration strategy. The superior performance of the improved algorithm has been verified by the comparison of optimization results given by each algorithm and the results of full wave simulation. The results indicate that the proposed technique could comfortably outperform PSO, HHO, SA, BWO and WOA in the non-uniform spiral antenna arrays synthesis problems. The simulation results of rectangular microstrip patch arrays indicate the effectiveness and reliability of the algorithm.

**Author Contributions:** Conceptualization, T.L. and Y.Y. (Yang Yang); methodology, T.L. and Y.Y. (Yang Yang); validation, T.L.; investigation, C.Z., F.C., X.L. and H.H.; data curation, T.L., Z.L. and Y.Y. (Yali Yao); writing—original draft preparation, T.L.; writing—review and editing, Y.Y. (Yang Yang). All authors have read and agreed to the published version of the manuscript.

**Funding:** This research was funded by Hefei City unveils major projects (grant number 2022SZD004) and National Key Project (grant GJXM92579).

**Data Availability Statement:** The data presented in this study are available on request from the corresponding author.

**Conflicts of Interest:** The authors declare no conflicts of interest.

## References

1. Karasev, A.S.; Stepanov, M.A. Genetic Algorithm for Antenna Array Thinning with Minimization of Side Lobe Level. In Proceedings of the 2021 XV International Scientific Conference on Actual Problems of Electronic Instrument Engineering (APEIE), Novosibirsk, Russia, 19–21 November 2021.
2. Dai, D.; Yao, M.; Ma, H.; Jin, W.; Zhang, F. An Asymmetric Mapping Method for the Synthesis of Sparse Planar Arrays. *IEEE Antennas Wirel. Propag. Lett.* **2018**, *17*, 70–73. [[CrossRef](#)]
3. Dawood, H.S.; El-Khobby, H.A.; Elnaby, M.M.A.; Hussein, A.H. Optimized VAA Based Synthesis of Elliptical Cylindrical Antenna Array for SLL Reduction and Beam Thinning Using Minimum Number of Elements. *IEEE Access* **2021**, *9*, 50949–50960. [[CrossRef](#)]
4. Tian, X.; Wang, B.; Tao, K.; Li, K. An Improved Synthesis of Sparse Planar Arrays Using Density-Weighted Method and Chaos Sparrow Search Algorithm. *IEEE Trans. Antennas Propag.* **2023**, *71*, 4339–4349. [[CrossRef](#)]
5. Sun, Y.; Sun, J.; Ye, L.; Selleri, S. Synthesis of Thinned Planar Concentric Circular Antenna Arrays Using a Modified Artificial Bee Colony Algorithm. *Int. J. Antennas Propag.* **2023**, *2023*, 7735267. [[CrossRef](#)]
6. Wang, B.; Tian, X.; Tao, K.; Neshati, M.H. Synthesis of Sparse Uniformly Excited Concentric Ring Arrays Using the Chaos Sparrow Search Algorithm. *Int. J. Antennas Propag.* **2023**, *2023*, 2926111. [[CrossRef](#)]
7. Diao, J.; Kunzler, J.W.; Warnick, K.F. Sidelobe Level and Aperture Efficiency Optimization for Tiled Aperiodic Array Antennas. *IEEE Trans. Antennas Propag.* **2017**, *65*, 7083–7090. [[CrossRef](#)]
8. Niccolai, A.; Zich, R.; Beccaria, M.; Pirinoli, P. SNO Based Optimization for Shaped Beam Reflectarray Antennas. In Proceedings of the 2019 13th European Conference on Antennas and Propagation (EuCAP), Krakow, Poland, 31 March–5 April 2019.
9. Reddy, K.Y.; Kumar, R.B.; Jijenth, M.; Suman, K.K.; Gangwar, V.S.; Singh, A.K. Synthesis of randomly spaced planar antenna array with low peak side lobe level (PSLL) using Modified Genetic Algorithm. In Proceedings of the 2017 IEEE International Conference on Antenna Innovations & Modern Technologies for Ground, Aircraft and Satellite Applications (iAIM), Bangalore, India, 24–26 November 2017.
10. Schlosser, E.R.; Tolfo, S.M.; Heckler, M.V.T. Particle Swarm Optimization for antenna arrays synthesis. In Proceedings of the 2015 SBMO/IEEE MTT-S International Microwave and Optoelectronics Conference (IMOC), Porto de Galinhas, Brazil, 3–6 November 2015.
11. He, X.; Alistarh, C.; Podilchak, S.K. Optimal MIMO Sparse Array Design Based on Simulated Annealing Particle Swarm Optimization. In Proceedings of the 2022 16th European Conference on Antennas and Propagation (EuCAP), Madrid, Spain, 27 March–1 April 2022.
12. Penghan, X.; Chen, K.; He, Z. Synthesis of thinned conical arrays using simulated annealing algorithm. In Proceedings of the 2009 International Conference on Communications, Circuits and Systems, Milpitas, CA, USA, 23–25 July 2009.
13. Owoola, E.O.; Xia, K.; Wang, T.; Umar, A.; Akindele, R.G. Pattern Synthesis of Uniform and Sparse Linear Antenna Array Using Mayfly Algorithm. *IEEE Access* **2021**, *9*, 77954–77975. [[CrossRef](#)]
14. Hu, H.; Li, H.; Liang, G.; Zhao, L.; Yang, J.; Wei, X. Phase-Only Pattern Synthesis for Spaceborne Array Antenna Based on Improved Mayfly Optimization Algorithm. *Electronics* **2023**, *12*, 895. [[CrossRef](#)]
15. Zhao, K.; Liu, Y.; Hu, K. Optimal Pattern Synthesis of Linear Array Antennas Using the Nonlinear Chaotic Grey Wolf Algorithm. *Electronics* **2023**, *12*, 4087. [[CrossRef](#)]
16. Heidari, A.A.; Mirjalili, S.; Faris, H.; Aljarah, I.; Mafarja, M.; Chen, H. Harris hawks optimization: Algorithm and applications. *Future Gener. Comput. Syst.* **2019**, *97*, 849–872. [[CrossRef](#)]
17. González, Á. Measurement of Areas on a Sphere Using Fibonacci and Latitude–Longitude Lattices. *Math. Geosci.* **2009**, *42*, 49–64. [[CrossRef](#)]
18. Fang, S.; Xue, Z.; Li, W.; Ren, W. Grating Lobe Suppression of Planar Array with Large Inter-Element Spacing by Using Genetic Algorithm. In Proceedings of the 2018 International Conference on Microwave and Millimeter Wave Technology (ICMMT), Chengdu, China, 7–11 May 2018.
19. Zhong, C.; Li, G.; Meng, Z. Beluga whale optimization: A novel nature-inspired metaheuristic algorithm. *Knowl.-Based Syst.* **2022**, *251*, 109215. [[CrossRef](#)]
20. Mirjalili, S.; Lewis, A. The Whale Optimization Algorithm. *Adv. Eng. Softw.* **2016**, *95*, 51–67. [[CrossRef](#)]

**Disclaimer/Publisher’s Note:** The statements, opinions and data contained in all publications are solely those of the individual author(s) and contributor(s) and not of MDPI and/or the editor(s). MDPI and/or the editor(s) disclaim responsibility for any injury to people or property resulting from any ideas, methods, instructions or products referred to in the content.